Available online at www.sciencedirect.com

SCIENCE DIRECT®

Journal of Molecular Catalysis A: Chemical 199 (2003) 73–84

JOURNAL OF MOLECULAR CATALYSIS A: CHEMICAL

www.elsevier.com/locate/molcata

Preparation of supported gold catalysts by gas-phase grafting of gold acethylacetonate for low-temperature oxidation of CO and of H_2

Mitsutaka Okumura [a,*], Susumu Tsubota [a], Masatake Haruta [b]

[a] *National Institute of Advanced Industrial Science and Technology, AIST Kansai, Midorigaoka 1-8-31, Ikeda, Osaka 563-8577, Japan*
[b] *National Institute of Advanced Industrial Science and Technology, AIST Tsukuba West, Onogawa 16-1, Tsukuba, Ibaraki 305-8569, Japan*

Received 2 April 2002; received in revised form 7 September 2002; accepted 7 September 2002

Abstract

In order to clarify the support effect on CO oxidation over Au catalysts without the influence of the size effect of Au, Au was deposited on a variety of supports with high dispersion by gas-phase grafting (GG) of an organo-gold complex. Comparison of Au/SiO_2 with Au/Al_2O_3 and Au/TiO_2, which were prepared by both GG and liquid-phase methods and were active for CO oxidation at 273 K, showed that there were no appreciable differences in their catalytic activities as far as Au is deposited as nanoparticles with strong interaction. However, Au deposited onto the acidic supports, such as silica–alumina and activated carbon (AC), exhibited a much lower CO oxidation catalytic activity than those of the active Au catalysts, such as Au/TiO_2.

Keywords: Au catalyst; Gas-phase grafting method; CO oxidation; Size effect; Support effect

1. Introduction

We have already reported that Au shows surprisingly high activity for CO oxidation at low temperatures when it is deposited as nanoparticles on select metal oxides [1,2]. Coprecipitation (CP) [2–4], deposition–precipitation (DP) [1,5] and co-sputtering [6], liquid-phase grafting [7] can produce highly dispersed Au catalysts, which exhibit unique catalytic nature in many different reactions depending on the type of metal oxide supports [8,9]. Another liquid-phase preparation method was also reported by Iwasawa and his coworkers [10]. In CO oxidation, the oxides of 3d transition metals, especially of group VIII, and hydroxides of alkaline earth metals [11,12] lead to high activities even at a temperature as low as 203 K. The requirements for the size of Au particles differ between the former and the latter supports. With TiO_2, Fe_2O_3 and Co_3O_4 supports, for example, Au particles in the range of 2–10 nm in diameter exhibit high activity, but by contrast only gold clusters smaller than 1.0 nm [13] exhibit high activity with $Be(OH)_2$ and $Mg(OH)_2$ supports.

Thus, when gold is deposited on the select metal oxides by liquid-phase methods, the catalytic activity is remarkably enhanced and can be measured in a fixed-bed flow reactor. Metal oxides suitable as a support are limited to a group of reducible metal oxides having *p*-type or *n*-type semiconductivities. In fact, Au supported on insulating, covalent bonded metal oxides, such as Al_2O_3 and SiO_2 was less active than Au/TiO_2, Au/Fe_2O_3, Au/Co_3O_4, and Au/NiO.

* Corresponding author. Tel.: +81-727-51-9832; fax: +81-727-51-9714.
E-mail address: m.okumura@aist.go.jp (M. Okumura).

1381-1169/03/$ – see front matter © 2003 Elsevier Science B.V. All rights reserved.
doi:10.1016/S1381-1169(03)00020-7

It should also be noted that the catalytic activity of Au/TiO_2 for CO oxidation markedly changes depending on preparation methods. Turnover frequency (TOF) differs by as much as 4 orders of magnitude between deposition precipitation and photodeposition [14]. An impregnation (IMP) method usually yields poorly active gold catalysts [14], however, it has been reported that a specific sequence of pretreatments (H_2 reduction at 773 K, calcination in 20 vol.% O_2 at 673 K, and then H_2 reduction at 473 K) appreciably enhances the catalytic activity of Au/TiO_2 [15]. Based on our experiences, [16–18] the above pretreatments are considered to be effective to evaporate chloride ion and sinter gold particles resulting in the stronger hetero-junction, to oxidize Au-TiO_2 interface, and to moisten the catalyst surface by H_2O produced by low-temperature H_2 reduction.

Taking these results into account, we have been led to believe that for the genesis of high activity of Au catalysts, the contact structure between Au particles and support is more important than the mean diameter of Au particles. Liu and Vannice have reported that the deposition of TiO_2 onto the surface of Au markedly enhances the catalytic activity for CO oxidation [16].

Furthermore, the preparation of highly dispersed Au catalysts, such as Au supported on an acidic support (e.g. silica–alumina), and Au supported on non-metal-oxide support (e.g. activated carbon (AC)), is much more difficult than that of Au/TiO_2 because there is no suitable preparation method for them.

In the present work, we have attempted to deposit gold on Al_2O_3, SiO_2, MCM-41, TiO_2, SiO_2–Al_2O_3 and active carbon by gas-phase grafting (GG) of an organo-gold complex in order to make the support effect in CO oxidation over Au catalysts clear. TG–TDA and FT-IR analyses were also conducted to examine the adsorption state and the decomposition of $Me_2Au(acac)$ on the support. Ab initio density functional theory (DFT) calculations were also performed to estimate the electronic structure of the gold precursor.

2. Experimental

2.1. Catalyst preparation

The metal oxides used as a support are Al_2O_3 powder (a reference sample of the Catalysis Society of Japan, JRC-ALO7, 180 m^2/g), SiO_2 powder (Fujisilycia Chemical Ltd., type G, specific surface area 310 m^2/g), MCM-41 (mesopore widths: 2.2, 2.7, 3.1 nm, specific surface area 1010, 1036, and 979 m^2/g), amorphous TiO_2 (Idemitsu Kosan Co. Ltd., 113 m^2/g), SiO_2–Al_2O_3 (JRC-SAH-1; Al_2O_3 assay 26.8%, 240 m^2/g, JRC-SAL-2; 13.8% 200 m^2/g) and AC, (Kansai Coke and Chemicals Co. Ltd., Maxsorb., 2000 m^2/g). As a gold precursor, $(CH_3)_2Au(CH_3COCH_2COCH_3)$, (abbreviated hereafter to $Me_2Au(acac)$), was used without further purification of the reagent available from Tri Chemical Laboratory Inc. Its vapor pressure at room temperature is approximately 8.5×10^{-3} Torr.

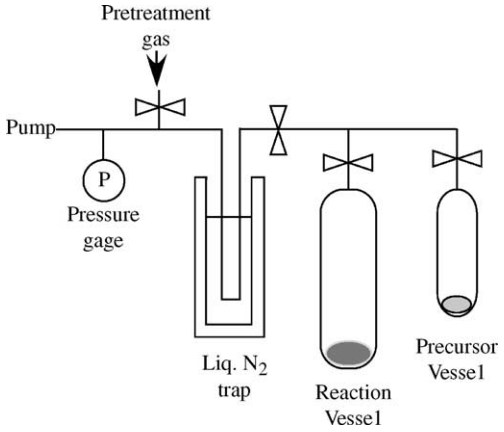

Fig. 1. Schematic diagram of the reaction apparatus for the gas-phase grafting method.

Fig. 1 shows the GG experimental setup, made of hard glass. The lowest pressure that could be reached in the apparatus was approximately 10^{-3} Torr. Support metal oxides were evacuated at 473 K for 4 h to remove water physically adsorbed and were then treated with 20 Torr oxygen at 473 K for 30 min to remove organic residue and to oxidize the surface. The precursor vessel was heated to a fixed temperature of 306 K to gradually evaporate a measured amount of $Me_2Au(acac)$. The precursor adsorbed on the metal oxide supports that were mounted in the reaction vessel was calcined in air at a fixed temperature in the range of 473–773 K to decompose into metallic gold particles on the support surface.

For comparison, Au/Al_2O_3, Au/SiO_2, and Au/TiO_2 catalysts were also prepared by the liquid-phase methods, CP, IMP, or DP using $HAuCl_4$ as a starting

reagent. They were finally calcined in air at 673 K. The Au/SiO_2 catalyst prepared by IMP was washed with hot water after calcinations in air to remove chloride ion and then dried at 393 K.

2.2. Catalyst characterization

The charge density of gold precursor was obtained by ab initio density functional calculations using the Gaussian 98 program [19]. For DFT calculations, the Becke 88 functional was used as an exchange functional and the Lee, Yang, and Parr (LYP) functional was used as a correlation functional. The basis sets used in these calculations were the double zeta effective core potential basis set (Lanl2DZ) on Au atom and the Dunning/Huzinaga full double zeta basis set (D95) on H, C, and O atoms.

TG–DTA analysis for $Me_2Au(acac)$ alone and $Me_2Au(acac)$ adsorbed on SiO_2 were performed by using RIGAKU TG8101D in the temperature range from 300 to 873 K in air. The state of adsorption and decomposition of $Me_2Au(acac)$ on the SiO_2 surface was monitored by means of FT-IR (Nicolet 20SXC).

The dispersion of gold particles was observed with a transmission electron microscope (TEM, Hitachi H-9000). At least 100 particles were chosen to determine the mean diameter of gold particles and the diameter distribution was obtained by using a computerized image analyzer (EXCEL, Nippon Avionics Co. Ltd.).

2.3. Catalytic activity measurements

All the catalytic activity measurements for CO oxidation and H_2 oxidation were performed by using a conventional fixed-bed flow reactor and by passing the reactant gas. A powder sample (100 mg) sieved between 70 and 120 mesh (212–125 μm) was placed on a ceramic wool plug in a quartz tube with an inner diameter of 6 mm. After the pretreatment of the catalyst samples in an air stream at 523 K for 30 min, the reactant gas (1 vol.% CO in air or 1 vol.% H_2 in air) was passed through the catalytic bed at a flow rate of 33 ml/min (SV = 20,000 h^{-1} ml/g catalyst). The catalyst temperature was monitored with a quartz-tube covered thermocouple in contact with the inlet part of the catalyst bed. It was raised or lowered stepwise and maintained at each temperature for more than 40 min until steady state conversions were obtained. Oxygen, nitrogen and carbon monoxide in the inlet and the outlet were analyzed by a gas chromatograph (Shimadzu GC-8A) with a thermal conductivity detector (TCD) and with a column of molecular sieve 13 × 5 m at 333 K. Calibration was done with a standard gas containing known concentrations of the components.

The activation energies were determined by Arrhenius plots. A powder catalyst sample (20–30 mg) mixed with quartz powder, both sieved between 70 and 120 mesh, was used for activity measurements. The flow rate of reactant gas (1 vol.% CO in air) and catalyst temperature was varied to keep the CO conversion between 10 and 20%. As the rate of CO oxidation was almost independent of the concentrations [5] of CO and O_2, it was calculated based on a zeroth order reaction.

The number of gold atoms exposed to the surface was calculated from the mean diameter of Au particles and the actual Au loading obtained with an inductively coupled plasma spectrometer (Sumika Chemical Analysis Service Co. Ltd.). Turnover frequency was calculated by dividing the reaction rate with the number of surface gold atoms.

3. Results and discussion

3.1. Adsorption and decomposition of Au precursor

In order to examine the charge distribution and the molecular structure of $Me_2Au(acac)$, ab initio DFT calculation was performed. Fig. 2a shows the charge density of $Me_2Au(acac)$. From the geometry optimization of $Me_2Au(acac)$, it was found that the molecular structure was almost plane. The signs of atomic charges change alternately on the acethylacetonate ligand and the large negative charges are observed on the oxygen atoms. These results suggested that $Me_2Au(acac)$ could be adsorbed onto the support surface without steric hindrance and the interaction between the gold precursor and the support surface might occur between $Me_2Au(acac)$ and the surface defect sites and/or the surface OH group.

The TG–DTA analysis for $Me_2Au(acac)$ and $Me_2Au(acac)$ absorbed SiO_2 were performed in order to examine the thermal stability of this precursor. In the DTA curve of $Me_2Au(acac)$ shown in Fig. 3a, two peaks are observed. The first endothermic peak

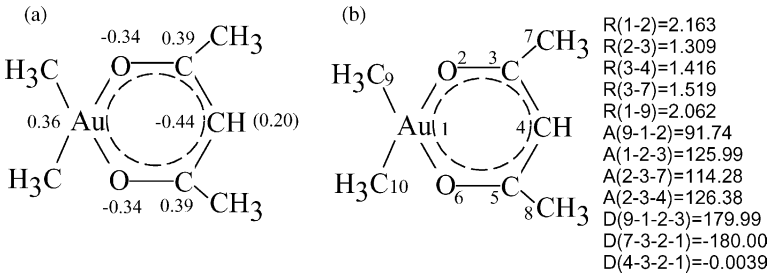

Fig. 2. Schematic diagram of (a) the charge density and (b) the geometry of $Me_2Au(acac)$. *R*: inter atomic length in Å; *A*: angle in degree; *D*: dihedral angle in degree.

at 355 K is due to the melting of $Me_2Au(acac)$ and the second exothermic peak at temperatures above 400 K can be ascribed to the decomposition of the gold precursor. This peak is a little tilted to the higher temperature side because the large exothermicity of the reaction resulted in a sharp increase in the sample temperature. The TG curve shows a gradual decrease from 353 K and reaches a steady value above 473 K, indicating that the decomposition of $Me_2Au(acac)$ is complete at 473 K. While the theoretical weight loss is calculated to be 39%, the weight loss observed was approximately 70%. This is probably because of the vaporization of part of the $Me_2Au(acac)$ during the heating procedure.

For $Me_2Au(acac)$ adsorbed on SiO_2, as shown in Fig. 3b, three peaks are observed. The first sharp exothermic peak that is observed at a temperature a little lower than that of $Me_2Au(acac)$ itself can be ascribed to the decomposition of the gold precursor. It appears that the decomposition might be enhanced on the SiO_2 surface. The second and third exothermic peaks are considered to be due to the combustion of the ligand residues. The decomposed residues might remain on the support surface up to 573 K. This suggests that calcination at a temperature above of 573 K is needed to prepare Au catalysts. The gradual decrease in weight in the TG curve above 573 K is due to the dehydration of SiO_2 itself, as the same tendency is observed in the case of SiO_2 alone.

Fig. 4a shows the FT-IR spectra of unsupported $Me_2Au(acac)$. Several peaks are observed in the range of 2800–3000 cm^{-1} and of 1000–1600 cm^{-1}. The

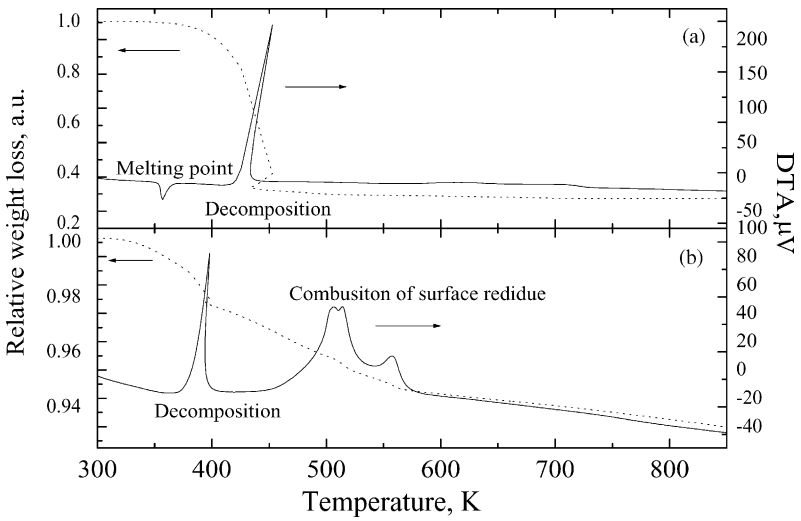

Fig. 3. TG–DTA curves of (a) $Me_2Au(acac)$ and (b) $Me_2Au(acac)$ adsorbed on the SiO_2 surface.

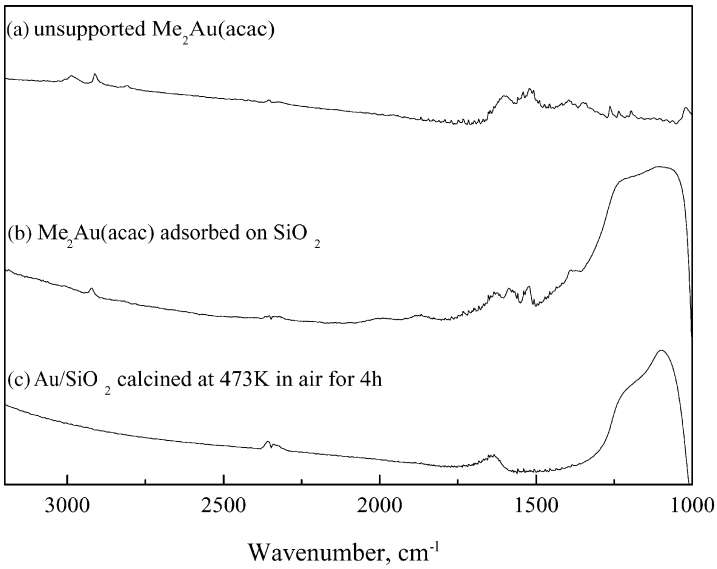

Fig. 4. IR spectra of (a) unsupported $Me_2Au(acac)$, (b) $Me_2Au(acac)$ adsorbed on SiO_2 surface and (c) Au/SiO_2 calcined at 473 K in air for 4 h.

former peaks are due to the C–H stretching of $–CH_3$ groups and of the C–H group of $Me_2Au(acac)$ and the latter peaks are due to the vibration modes of acetylacetonate ligand.

Fig. 4b shows the FT-IR spectra of silica-supported $Me_2Au(acac)$, which are not so different from that of the unsupported $Me_2Au(acac)$. The spectra showed a band at ca. 1600–1680 cm^{-1} that is due to water physically adsorbed on the support surface at room temperature. These FT-IR spectra resemble the spectra of silica-supported $Pt(acac)_2$ reported by Kohler et al. [21]. $Me_2Au(acac)$ absorbed on the SiO_2 surface might be weakly interacted and maintain its original structure. In Fig. 4c, the FT-IR spectra of silica-supported $Me_2Au(acac)$ obtained after calcination in air at 473 K showed no peaks related to

Table 1
Mean diameters of gold particles in Au supported on Al_2O_3, SiO_2, and TiO_2 and their kinetic parameters for the oxidation of H_2 and of CO

Support	Method	Au loading (wt.%)	Calculated temperature (K)	Mean diameter of Au (nm)	$T_{1/2}$ (H_2) (K)	$T_{1/2}$ (CO) (K)	TOF (CO) (273 K) (s^{-1})	E_a (CO) (kJ/mol)
Al_2O_3	GG[a]	5.3	573	3.5 ± 2.7[b]	331	261	0.01	36
	DP[c]	0.94	573	2.4 ± 1.1[b]	362	290	0.02	32
	CP[d]	4.2	673	3.5 ± 1.9[b]	367	289	0.006	38
SiO_2	Gg[a]	6.6	673	6.6 ± 3.8[b]	329	227	0.02	17
	IMP[e]	14.7	673	20[f]	589	668	–	–
TiO_2	GG[a]	4.7	573	3.8 ± 2.7[b]	321	239	0.02	41
	DP[c]	2.0	573	1.7 ± 0.4[b]	313	237	0.06	37

Turn over frequency of CO oxidation at 273 K, E_a (CO): activation energy of CO oxidation.
[a] Gas-phase grafting.
[b] TEM observation.
[c] Deposition–precipitation.
[d] Coprecipitaion.
[e] Impregnation.
[f] XRD measurement.

$Me_2Au(acac)$ compound. This result together with TG–DTA results indicate that the ligand was already decomposed or vaporized during the calcination at 473 K for 4 h but partly remained as carbon residues.

3.2. Comparison of catalytic activity among Au/Al_2O_3, Au/SiO_2, and Au/TiO_2 prepared by different methods

Table 1 lists the catalytic properties of Au/Al_2O_3, Au/SiO_2, and Au/TiO_2 prepared by GG and other methods including temperatures for 50% conversion ($T_{1/2}$) of CO and of H_2. Because the optimum calcination temperature depends on support metal oxides and preparation methods, the catalyst precursors were calcined in air at 573 or 673 K. Hydrogen oxidation takes place at lower temperatures than CO oxidation over unsupported gold powder [2] and appears to be much less influenced by metal-support interaction. Therefore, the catalytic activity for H_2 oxidation can be primarily related to the exposed surface area of gold. Conversely, the catalytic activity for CO oxidation is markedly dependent on a combination of the preparation method [14], the mean diameter of Au particles [1], and the contact structure between the Au particles and the support metal oxides [5,20].

For all the three supports, GG method produced highly active catalysts for CO oxidation. While the coprecipitation method is advantageous in preparing powder catalysts with high Au loadings above 10 wt.%, with an intermediate Au loading below 5 wt.% it resulted in lower catalytic activity than the other methods. The $T_{1/2}$ value of Au/Al_2O_3 prepared by CP is higher than that of the GG sample and is similar to that of the DP sample with a much lower Au loading.

TEM photographs in Fig. 5a shows that many small gold particles are dispersed on Al_2O_3 by GG but a few large gold particles are also observed. The mean diameter of the Au/Al_2O_3 by GG is 3.5 ± 2.7 nm. While the mean diameter of Au particles is almost the same as that of the CP sample, this standard deviation of Au particles is much larger than those for Au/Al_2O_3 prepared by coprecipitation and deposition–precipitation. This tendency is the same with that of Au/TiO_2.

In contrast to other supported gold catalysts, Au/SiO_2 (IMP), which is poorly active for both H_2 and CO oxidation (much higher $T_{1/2}$ values), exhibits

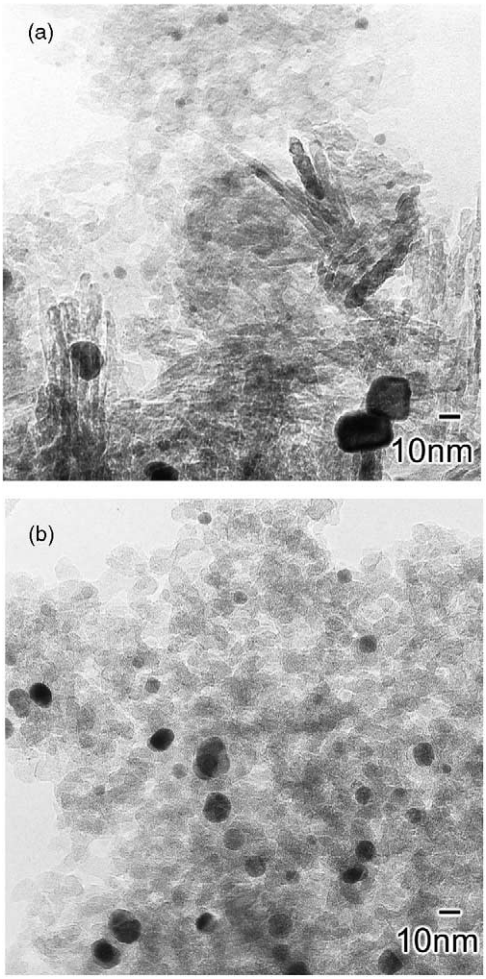

Fig. 5. TME images of (a) Au/Al_2O_3 prepared by GG and (b) Au/SiO_2 prepared by GG and calcined in air at 673 K for 4 h.

catalytic nature similar to unsupported Au particles; the catalytic activity for H_2 oxidation is higher than that for CO oxidation. Because the catalytic activities of Au/SiO_2 for both the reactions were too low with small Au loadings, Table 1 shows the data for the sample with a high Au loading. Conversely, Au/SiO_2 (GG) exhibits high catalytic activity and $T_{1/2}$ values are lower by approximately 100 K for CO oxidation than for H_2 oxidation. It can be assumed that using the GG method, nanoparticles of Au can be deposited with strong interaction even on SiO_2 support.

In the TEM photograph in Fig. 5b for Au/SiO_2 (GG) calcined at 673 K, most of the Au particles are smaller than 10 nm in diameter. The mean diameter is

calculated to be 6.6 nm, which is smaller than that of Au/SiO_2 (IMP) by a factor of three.

Although Au loading differs in TiO_2-supported catalysts, judging from $T_{1/2}$ values for both CO oxidation and H_2 oxidation, GG can be regarded to be as effective as DP in the preparation of highly dispersed Au particles. Au/TiO_2 prepared by photochemical deposition [16] or by mechanical mixing of Au colloids [5,20] with TiO_2 powder have spherical Au particles simply loaded on the TiO_2 support and exhibits poor catalytic activities for CO oxidation. However, calcination at higher temperatures gives higher catalytic activities for the mechanically mixed Au colloid. These results suggest that the Au-support interaction and, more definitely, an increase in peripheral distance between Au particles and support may have a key role for the genesis of remarkably high catalytic activities in CO oxidation at low temperatures.

The Arrhenius plots are depicted in Fig. 6. From the straight lines, rates of reaction and TOF for CO oxidation at 273 K were obtained. While the gas adsorption technique is generally used to determine the number of surface active sites of Pt, no reliable method is available for determining the exposed surface area of Au. TEM observation can be used instead of the above technique as long as the dispersion of Au particles is homogeneous. Because it was probable that we missed the existence of small Au particles that could not be clearly observed by TEM and therefore the mean diameters of gold particles were not always decisively correct, TOF values should be only roughly compared. A little larger TOF value for Au/TiO_2 (DP) can be ascribed to a smaller mean diameter of Au particles, which is in accordance with our previous results [1].

The apparent activation energies of Au/Al_2O_3 prepared by the three methods are almost identical. TOF values of the GG and DP samples are also in the same order. While Au/Al_2O_3 catalysts prepared by CP and by GG have almost the same Au loadings and mean diameters of Au particles, TOF of the GG sample are higher than that of the CP sample. It is likely that Au particles are partly embedded in the bulk of the Al_2O_3 support in the CP sample.

The TOF and activation energy of Au/SiO_2 (IMP) were not obtained because the catalyst was inactive at 273 K. In contrast, Au/SiO_2 prepared by using the GG method exhibits catalytic activity for CO oxidation as high as Au/Al_2O_3 and Au/TiO_2, with an activation energy of 17 kJ/mol and TOF at 273 K of 0.02 s^{-1}. It should be noted that the apparent activation energy

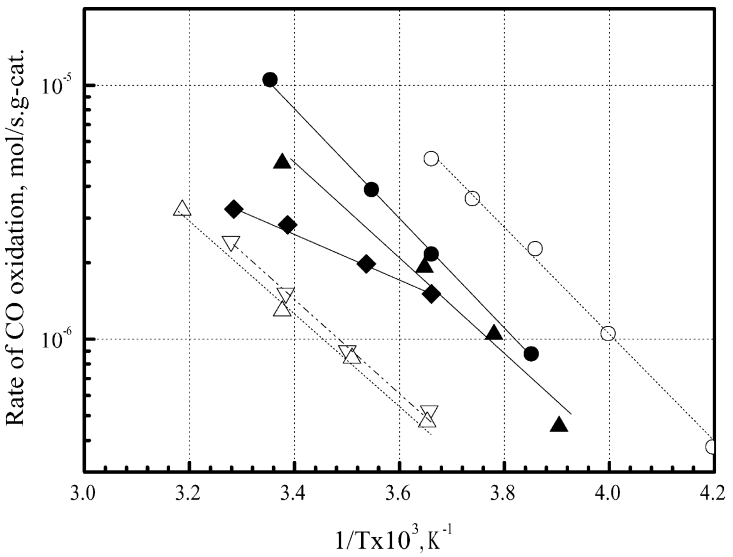

Fig. 6. Logarithmic reaction rate of CO oxidation over Au/Al_2O_3, Au/SiO_2, and Au/TiO_2 as a function of reciprocal temperature. The temperature for calcination is the same as that in Table 1. (▲): 5.3 wt.% Au/Al_2O_3 by GG; (△): 0.96 wt.% Au/Al_2O_3 by DP; (▽): 4.2 wt.% Au/Al_2O_3 by CP, (◆): 6.6 wt.% Au/SiO_2 by GG, (●): 4.7 wt.% Au/TiO_2 by GG, (○): 2.0 wt.% Au/TiO_2 by DP.

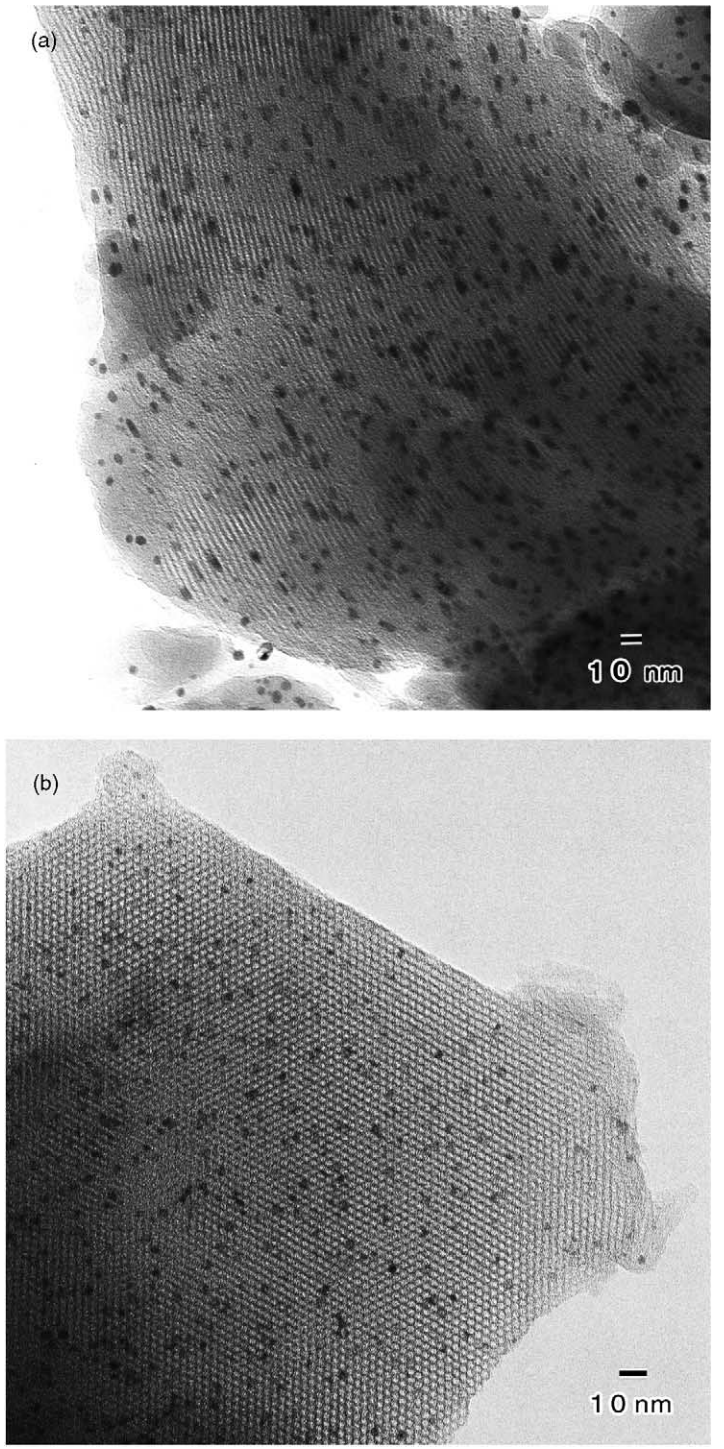

Fig. 7. TEM images of Au/MCM-41 prepared by GG and calcined in air at 673 K for 4 h.

Table 2
Mean diameters of gold particles and kinetic parameters of CO and H_2 oxidation for Au supported on MCM-41

Catalyst[a]	Method	Au[b] (wt.%)	D_{Au} (nm)	CO oxidation			H_2 oxidation
				$T_{1/2}$ (K)	E_0 (kJ/mol)	TOF[c] (s^{-1})	$T_{1/2}$ (K)
Au/MCM-41 (22 Å)	GG[d]	4.2	4.2 ± 1.4[e]	263	26	0.02	303
Au/MCM-41 (27 Å)	GG[d]	2.9	4.0 ± 1.5[e]	259	27	0.05	302
Au/MCM-41 (31 Å)	GG[d]	3.5	4.9 ± 1.9[e]	264	23	0.04	310
Au/SiO_2	GG[d]	6.6	6.6 ± 3.8[e]	227	17	0.02	329
Au/SiO_2	IMP[f]	14.7	20.0[g]	477	–	–	357
Au/MCM-41 (22 Å)	IMP[f]	6.8	16.1[g]	608	–	–	380

[a] Calcined in air at 673 K for 4 h.
[b] ICP analysis.
[c] Turnover frequency at 273 K.
[d] Gas-phase grafting.
[e] TEM observation.
[f] Impregnation.
[g] XRD measurement.

for Au/SiO_2 (GG) is lower than those for Au/Al_2O_3 and Au/TiO_2, 30–40 kJ/mol and larger than that for unsupported Au powder [22].

The activation energies and TOF at 273 K are similar between the two Au/TiO_2 catalysts prepared by the GG and by DP methods. As the activation energy for Au/SiO_2 is lower than those of Au/Al_2O_3 and Au/TiO_2, the nature of metal oxide supports has some influence on the rate-determining step in the low-temperature CO oxidation, probably on the oxygen activation step.

From the results obtained for the Au catalysts prepared by GG, the order of TOF among Au/Al_2O_3, Au/SiO_2 and Au/TiO_2 could be compared and was found to be nearly the same. The extremely low catalytic activity of Au/SiO_2 (IMP) for CO oxidation was due to the large Au particles simply loaded on SiO_2 with a short contact perimeter distance.

3.3. Characteristic structure and catalytic properties of Au/MCM-41 prepared by GG

In order to examine the effect of the structured material for the deposition of Au nanoparticles by GG, MCM-41 was used for the support of Au catalyst. Fig. 7a shows a TEM photograph of Au deposited on MCM-41 (2.2 nm) by GG. Both dark rod-like images and spherical images are seen. The shorter width of rod-like particle was taken as the diameter of the rod-like particles. The mean diameter of all particles is 4.2 nm and that of the rod-like particles is 3.4 nm. The mean diameter and the most frequent diameter of rod-like Au particles in Fig. 7a are almost equivalent to the width of the d_{100} value (33.9 Å) that includes mesopore width and thickness of MCM-41 wall. Therefore, the apparent growth of Au rods or wires along with the channels of the support strongly suggests that

Table 3
$T_{1/2}$[CO] and mean diameters of Au particles (D_{Au}) in Au deposited on SiO_2–Al_2O_3, and AC

Support	Method	Au loading (wt.%)[a]	Calculated temperature (K)	D_{Au} (nm)[b]	$T_{1/2}$ (CO) (K)
SiO_2–Al_2O_3 (SAL-2)	GG[c]	3.0	673	6.9 ± 1.7	543
SiO_2–Al_2O_3 (SAH-1)	GG[c]	3.0	673	5.8 ± 4.1	618
AC	GG[c]	5.2	573	5.0 ± 1.6	<573
SiO_2	GG[c]	6.6	673	6.6 ± 3.8	227

[a] ICP analysis.
[b] TEM observation.
[c] Gas-phase grafting.

some amount of Au particles are incorporated into the channels of the MCM-41 support. Fig. 7b was also in good agreement with this interpretation as the small dots were located on the mesopore channels. It can also be seen that spherical and hemispherical Au particles are mostly deposited on the disordered parts of the MCM-41. The mean diameters of Au particles deposited by GG on MCM-41 with mesopore widths of 2.7 and 3.1 nm are 4.0 and 4.9 nm, respectively, and are much smaller than that of Au/SiO_2. This result shows that the fine ordered channel structure keeps the Au particles small.

The catalytic activities of Au/MCM-41 were examined for the oxidation of CO and of H_2. The results are summarized in Table 2. While Au/MCM-41 samples prepared by GG exhibit high catalytic activities for H_2 oxidation, Au/MCM-41 samples exhibit higher catalytic activities in CO oxidation than in H_2 oxidation. Furthermore, CO oxidation took place at temperatures below 273 K and the deactivation of the catalysts was not observed at 273 K for 4 h.

TOF values for CO oxidation at 273 K are in the same order as those for Au deposited on SiO_2 by GG and on TiO_2 by liquid-phase methods. It is likely that Au particles incorporated into the channel of MCM-41 do not participate in the reaction. The similar TOF values implies that Au particles incorporated deep into the mesopore channels do not constitute the majority. The smaller Au particles, especially those <30 Å, lead to a higher TOF.

Conversely, Au/MCM-41 prepared by IMP has poor dispersion of Au with a mean particle diameter of approximately 20 nm. It can oxidize only half of CO even at 608 K and exhibits much lower catalytic activity for CO oxidation than for H_2 oxidation, indicating weak interaction between Au particles and the support. The large differences between GG and IMP methods in both the mean diameter of Au particles and the catalytic activities are in accordance with the results obtained for Au/SiO_2.

3.4. CO oxidation over Au/silica–alumina and Au/AC prepared by GG

Table 3 summarized the mean diameters of Au particles (D_{Au}) of Au supported on SiO_2–Al_2O_3, and AC and their 50% conversion temperature in CO oxidation reaction ($T_{1/2}$). TEM images of Au/SiO_2–Al_2O_3

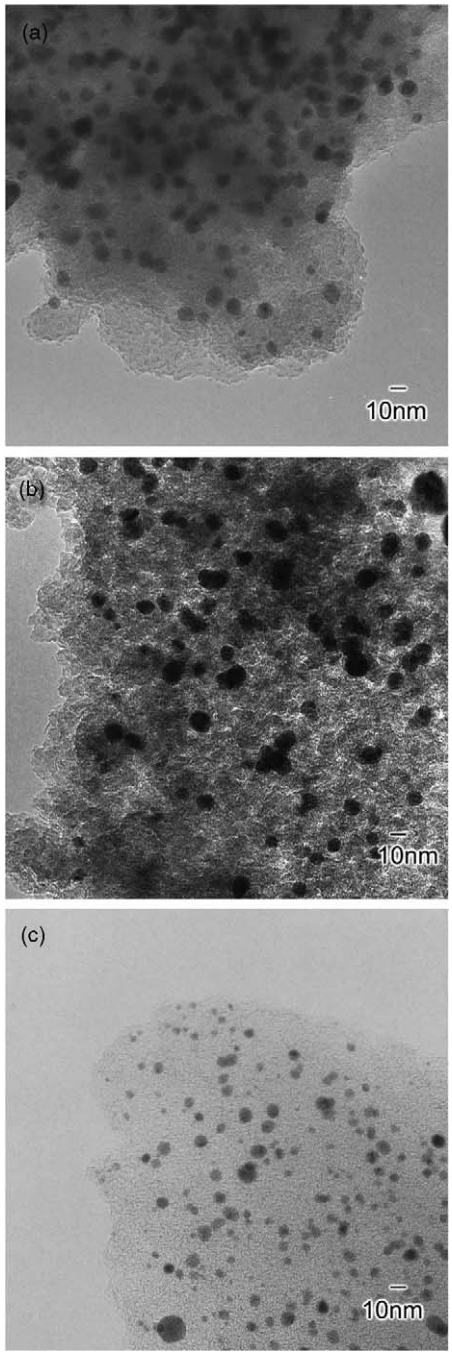

Fig. 8. TEM images of (a) Au/SAH-1 by GG and calcined in air at 673 K for 4 h, (b) Au/SAL-2 by GG and calcined in air at 673 K for 4 h and (c) Au/AC prepared by GG and calcined in air at 573 K for 4 h.

and Au/AC are shown in Fig. 8. The TEM images show that the mean diameter of Au particles deposited on these supports by GG are under 7 nm. Therefore, it was found that the support is not limited to select metal oxides when Au catalysts are prepared by GG method. Although D_{Au} of these catalysts were similar to that of Au/SiO_2 by GG, the catalytic activities of $Au/SiO_2–Al_2O_3$ and Au/AC were less active than others from the view point of $T_{1/2}$[CO]. This fact showed that an acidic support, such as $SiO_2–Al_2O_3$ and non-metal-oxide support, such as AC is not suitable for CO oxidation reaction. Consequently, it was found that the major controlling factors for the evolution of CO oxidation catalytic activity was the selection of supports as well as the size of Au particles on the support. The reducibility of the support (SiO_2 and Al_2O_3 versus TiO_2) does not make appreciable difference, however, acidity (SiO_2 versus $SiO_2–Al_2O_3$) is decisively important.

4. Conclusions

From the comparison of the catalytic activities for the oxidation of CO and of H_2 among Au/Al_2O_3, Au/SiO_2, Au/MCM-41, Au/TiO_2, $Au/SiO_2–Al_2O_3$, and Au/AC (activated carbon) prepared by GG and the liquid-phase methods, such as deposition–precipitation, the following conclusions have been derived.

1. Gold can be deposited on SiO_2, MCM-41, $Au/SiO_2–Al_2O_3$, and Au/AC as nano particles with high dispersion by the gas-phase grafting of an acetylacetonate complex of gold, while liquid-phase preparation methods are not effective to these supports.
2. In contrast to the previous knowledge that semiconductive metal oxides are preferable as a support, Au nanoparticles highly dispersed on SiO_2 and MCM-41 are also active for CO oxidation at temperatures below 273 K.
3. The order of TOF values for CO oxidation at 273 K are similar among Au/Al_2O_3, Au/SiO_2, and Au/TiO_2, indicating that the deposition of gold particles on the supports with strong interaction is a major controlling factor for the evolution of catalytic activity and that the semiconductive or reducible nature of the support is not a ruling factor for CO oxidation at 273 K.
4. The lower catalytic activities of $Au/SiO_2–Al_2O_3$ and Au/AC suggest that acidic supports and non-metal-oxide supports are the only exceptions in generating high catalytic activity for low-temperature CO oxidation.

References

[1] H. Haruta, S. Tsubota, T. Kobayashi, H. Kageyama, M.J. Genet, B. Delmon, J. Catal. 144 (1993) 175.
[2] M. Haruta, N. Yamada, T. Kobayashi, S. Iijima, J. Catal. 115 (1989) 301.
[3] S.D. Gardner, G.B. Hoflund, B.T. Upchurch, D.R. Schryer, E.J. Kielin, J. Schryer, J. Catal. 129 (1991) 114.
[4] A. Knell, P. Barnickel, A. Baiker, A. Wokaun, J. Catal. 137 (1992) 306.
[5] S. Tsubota, D.A.H. Cunningham, Y. Bando, M. Haruta, in: G. Poncelet, et al. (Eds.), Preparation of Catalysts VI, Elsevier, Amsterdam, 1995, pp. 227–235.
[6] T. Kobayashi, M. Haruta, S. Tsubota, H. Sano, Sens. Actuators B1 (1990) 222.
[7] M. Okumura, M. Haruta, Chem. Lett. (2000) 396.
[8] M. Haruta, Catal. Today 36 (1996) 153.
[9] M. Haruta, Catal. Surv. Jpn. 1 (1997) 61.
[10] Y.Z. Yuan, K. Asakura, H.L. Wan, K. Tsai, Y. Iwasawa, Catal. Lett. 42 (1996) 15.
[11] M. Haruta, T. Kobayashi, S. Tsubota, Y. Nakahara, Chem. Expr. 3 (1988) 159.
[12] S. Tsubota, M. Haruta, T. Kobayashi, A. Ueda, Y. Nakahara, in: G. Poncelet, et al. (Eds.), Preparation of Catalysts V, Elsevier, Amsterdam, 1991, pp. 695–704.
[13] W. Vogel, D.A.H. Cunningham, K. Tanaka, M. Haruta, Catal. Lett. 40 (1996) 175.
[14] G.R. Bamwenda, S. Tsubota, T. Nakamura, M. Haruta, Catal. Lett. 44 (1997) 83.
[15] S.D. Lin, M. Bollinger, M.A. Vannice, Catal. Lett. 17 (1993) 245;
Z.M. Liu, M.A. Vannice, Catal. Lett. 43 (1997) 51.
[16] M.A. Bollinger, M.A. Vannice, Appl. Catal. B 8 (1996) 417.
[17] M. Okumura, T. Tanaka, A. Ueda, M. Haruta, Solid State Ion. 95 (1997) 143.
[18] Y. Yuan, K. Asakura, H. Wan, K. Tsai, Y. Iwamoto, Chem. Lett. (1996) 755.
[19] M.J. Frisch, G.W. Trucks, H.B. Schlegel, G.E. Scuseria, M.A. Robb, J.R. Cheeseman, V.G. Zakrzewski, J.A. Montgomery Jr., R.E. Stratmann, J.C. Burant, S. Dapprich, J.M. Millam, A.D. Daniels, K.N. Kudin, M.C. Strain, O. Farkas, J. Tomasi, V. Barone, M. Cossi, R. Cammi, B. Mennucci, C. Pomelli, C. Adamo, S. Clifford, J. Ochterski, G.A. Petersson, P.Y. Ayala, Q. Cui, K. Morokuma, D.K. Malick, A.D. Rabuck, K. Raghavachari, J.B. Foresman, J. Cioslowski, J.V. Ortiz, B.B. Stefanov, G. Liu, A. Liashenko, P. Piskorz, I. Komaromi, R. Gomperts, R.L. Martin, D.J. Fox, T. Keith, M.A. Al-Laham, C.Y. Peng, A. Nanayakkara, C. Gonzalez, M. Challacombe,

P.M.W. Gill, B. Johnson, W. Chen, M.W. Wong, J.L. Andres, C. Gonzalez, M. Head-Gordon, E.S. Replogle, J.A. Pople, Gaussian Inc., Pittsburgh, PA, 1998.
[20] S. Tsubota, T. Nakamura, M. Haruta, Catal. Lett. 56 (1998) 131.
[21] S. Kohler, M. Peiche, S. Frobel, M. Baerns, in: G. Poncelet, et al. (Eds.), Preparation of Catalysts VI, vol. 1009, Elsevier, Amsterdam, 1995.
[22] Y. Iizuka, T. Tode, T. Takao, K. Yatsu, T. Takeuchi, S. Tsubota, M. Haruta, J. Catal. 189 (1999) 50.